Title: Nanoencapsulation and release study of enzymes from *Alkanivorax borkumensis* in chitosan-tripolyphosphate formulation

Authors: Tayssir Kadri, Agnieszka Cuprys, Tarek Rouissi, Satinder Kaur Brar, Rimeh Daghrir, Jean-Marc Lauzon

PII: S1369-703X(18)30158-X
DOI: https://doi.org/10.1016/j.bej.2018.05.013
Reference: BEJ 6950

To appear in: *Biochemical Engineering Journal*

Received date: 21-2-2018
Revised date: 26-4-2018
Accepted date: 14-5-2018

Please cite this article as: Kadri T, Cuprys A, Rouissi T, Brar SK, Daghrir R, Lauzon J-Marc, Nanoencapsulation and release study of enzymes from *Alkanivorax borkumensis* in chitosan-tripolyphosphate formulation, *Biochemical Engineering Journal* (2010), https://doi.org/10.1016/j.bej.2018.05.013

Nanoencapsulation and release study of enzymes from *Alkanivorax borkumensis* in chitosan-tripolyphosphate formulation

Tayssir Kadri[†], Agnieszka Cuprys[†], Tarek Rouissi[†], Satinder Kaur Brar[*†], Rimeh Daghrir[‡], Jean-Marc Lauzon[§]

[†]INRS-ETE, Université du Québec, 490, Rue de la Couronne, Québec, Canada G1K 9A9.

[‡]696, avenue Sainte Croix, Montréal (Québec) H4L 3Y2.

[§]TechnoRem Inc., 4701, rue Louis-B.-Mayer, Laval (Québec) - H7P 6G5.

***Corresponding author:** Tel: + 418 654 3116; Fax: + 418 654 2600; *E-mail*: satinder.brar@ete.inrs.ca

Graphical abstract

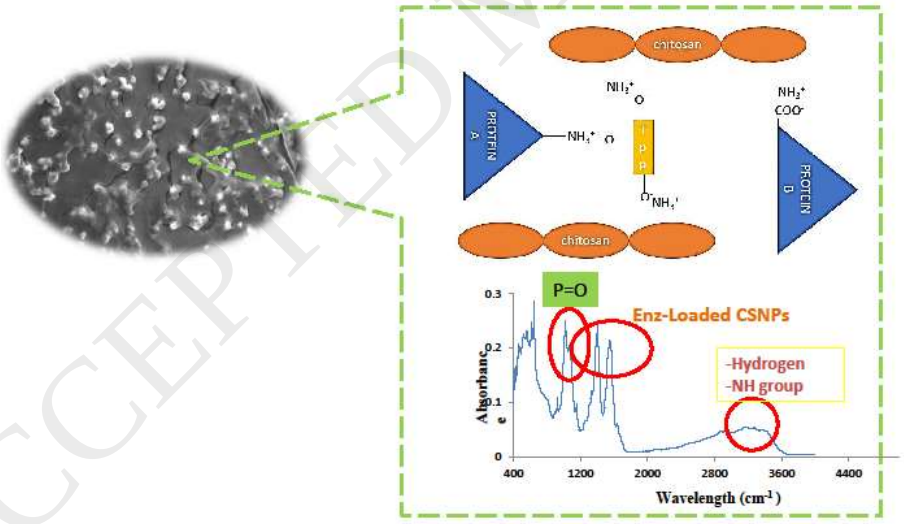

Highlights

- A successful nano-encapsulation of alkane hydroxylase and lipase in chitosan polymer.
- Different enzyme-chitosan/tripolyphosphate ratios were studied.
- (5:1) ratio was maintained for the best entrapment efficiency.
- The half-life of the immobilized enzymes was important, even after 30 days.

Abstract

The crude alkane hydroxylase and lipase enzymes from the hydrocarbonoclastic bacterium, *Alcanivorax borkumensis* were entrapped into chitosan nanoparticles (CSNPs) by ionotropic gelation method. For an optimal loading efficiency, enzyme-chitosan/tripolyphosphate (ENZ-CS/TPP) ratio was investigated. Fourier transform infrared spectra and morphology by scanning electron microscopy were used to explore and confirm alkane hydroxylase and lipase loaded into CSNPs. Seven consecutive ratios were investigated. Entrapment efficiency increased by increasing the ratio enzyme-chitosan/TPP. The optimal ratio with the best entrapment efficiency that was maintained for both alkane hydroxylase and lipase was 5:1. Particle size and zeta potential of the optimal ENZ-CSNPs was 473 nm and +21.8, respectively. Entrapment efficiency for alkane hydroxylase loaded CSNPs and lipase loaded CSNPs was 58.37% and 67.14%, respectively.

The immobilized alkane hydroxylase and lipase exhibited more than two folds increase in vitro half-life in comparison with the free enzymes maintaining around

70% of initial activity after 5 days. This study leads to a better understanding of how to prepare CSNPs, how to achieve high encapsulation efficiency and how to prolong the release of enzymes from CSNPs.

KEYWORDS: Nano-encapsulation; chitosan; *Alcanivorax borkumensis*; alkane hydroxylase; lipase.

1. Introduction

The ubiquitous usage of petroleum hydrocarbons (PHCs) has resulted in their frequent detection in soil and water which causes adverse effects on the ecosystem [1,2]. They affect the biota due to bioaccumulation, i.e. in plants or adipose tissues of animals [3,4]. Technologies, commonly used for soil remediation, are expensive and can lead to incomplete decomposition of contaminants [5]. Furthermore, PHCs do not degrade easily; hence the total and ultimate oil removal completely relies on bioremediation carried out by hydrocarbonoclastic bacteria that are key players . Importantly, *Alcanivorax borkumensis*, a rod-shaped marine γ-proteobacterium is able to grow on a highly restricted spectrum of substrates, predominantly alkanes and many studies have demonstrated its pivotal role in oil bioremediation [9–12]

. The genome of *A. borkumensis* has been completely sequenced [13], and many genes encoding for enzymes initiating the degradation of these hydrocarbons have been detected. The *A. borkumensis* alkane hydroxylase system is able to degrade a large range of alkanes up to C32 and branched aliphatics, as well as isoprenoid

hydrocarbons, alkylarenes and alkylcycloalkanes. This spectrum is much larger based on the knowledge about alkane hydroxylase complexes. This makes the choice to study alkane hydroxylase of a unique importance [13]. Furthermore, other than the extensive production of lipase by *A. borkumensis*, lipase demonstrates an important role in oily hydrocarbons biodegradation. In fact, lipase activity has been used as a biochemical parameter for testing hydrocarbon degradation and it is an excellent indicator to monitor the decontamination of a hydrocarbon polluted site [14].

The methods of immobilization of the enzymes, such as micro- and nano-encapsulation, have been widely investigated [15–22]. In encapsulation, the compound is immobilized and separated from the external environment with a semi-permeable membrane [23]. This technique may result in improvement of enzyme, pH and temperature stability. Moreover, , the advantage is the protection of biological material from unfavorable conditions in the external environment. Moreover, encapsulation of the enzyme may be the solution for the cost-effective system to eliminate the environmental contaminants [23].

In most of the reported investigations, pure and costly enzymes were employed while it is possible to use the crude enzyme, as in our case, it was a mix of crude alkane hydroxylase and crude lipase.

Chitosan (CS), a derivative form chitin, is a biopolymer widely used in different immobilization methods, such as the immobilization of methanotroph cells for the production of methanol reported by Patel et al., [24,25] or the encapsulation of strawberry polyphenols reported by Pulicharla et al., [26]. Its success is due to non-toxicity, biodegradability, biocompatibility, easy accessibility and low-cost

[23]. The generation of chitosan particles may be obtained in two ways [27]. The first involves the covalent bonds formed between chitosan and cross-linker, like glutaraldehyde. The other method uses the electrostatic interactions between positively charged CS and a negatively charged polyanion, e.g. commonly utilized tripolyphosphate (TPP).

There are several reports on the immobilization of enzymes on chitosan polymer. However, encapsulating enzymes from the interesting hydrocarbonoclastic bacteria *A. borkumensis* in chitosan nanoparticles is innovative and may provide a deeper knowledge of particle application on a petroleum hydrocarbon contaminated site. Hence, in this study, the optimization of enzymes encapsulation using chitosan nanoparticles generated by TPP and glutaraldehyde was studied. Enzymes release study, as well as kinetic of release, was performed and half-life was investigated.

2. Materials and methods

2.1 Materials

All chemical reagents of highest purity, such as high molecular weight chitosan (100-300 kDa), sodium tripolyphosphate (TPP), acetic acid (99.7%), hexadecane (99%), nicotinamide adenine dinucleotide phosphate (NADPH), Dimethyl sulfoxide (DMSO), *p*-nitrophenol (p-NP) and *p*-nitrophenyl palmitate (*p*-NPP) were purchased from Fisher Scientific or Sigma-Aldrich (Ontario, Canada). Phosphate buffer saline (PBS) and other reagents used were of analytical grade. The strain, *Alcanivorax borkumensis* was purchased from DSMZ (Braunschweig, Germany). Double distilled water (DDW) was produced in the laboratory using Milli-Q/Milli-Ro Millipore system (Massachusetts, USA).

2.2 Bacterial strain

Alcanivorax borkumensis strain SK2 (DSM 11573) was used in this study. *A. borkumensis* was sub-cultured and streaked on agar plates, incubated for 72 h at 30±1 °C and then preserved at 4±1 °C for future use. Standard media consisted of (per liter of distilled water): 23 g NaCl, 0.75 g KCl, 1.47 g $CaCl_2 . 2H_2O$, 5.08 g $MgCl_2. 6H_2O$, 6.16 g $MgSO_4. 7H_2O$, 0.89 g $Na_2HPO_4. 2H_2O$, 5 g $NaNO_3$, and 0.03 g $FeSO_4. 7H_2O$ [28]. The media was supplied with 3% (v v^{-1}) hexadecane as

the carbon and energy source and the growth was monitored at 30±1 °C, 150 rpm for 72h. Agar plates were prepared with the same media and agar was added at 18 g/L.

The enzymes used in this work were produced in controlled conditions of a 5 L bioreactor using 5% (v v^{-1}) of motor oil as sole carbon source for the growth of *Alcanivorax borkumensis*.All the details of this fermentation are explained in our previous work (unpublished data). Results of protein concentration, alkane hydroxylase activity and lipase activity obtained during the fermentation time are presented in Fig. S1.

2.3 Total protein assay

Total protein concentration was determined according to the Bradford [29] method. The principle of this assay is that the binding of protein molecules to Coomassie dye under acidic conditions results in a color change from brown to blue.

2.4 Sonication

A. borkumensis cell pellet (1 g) frozen at -20 °C was re-suspended in phosphate buffer (1 mL, 0.1 M, pH 8.0). The mixture was sonicated by using two frequencies of ultrasounds (22 kHz and 30 kHz) for 6 min at 4 °C and centrifuged at 13 000×g for 20 min. The supernatant was used as a crude intracellular enzyme extract.

2.5 Alkane hydroxylase assay

Alkane hydroxylase activity was measured using a cofactor (NADPH) depletion assay to determine relative activities. The supernatant containing the enzyme was diluted into phosphate buffer (0.1 M, pH 8), alkane substrate (0.5-1 mM), and

dimethyl sulfoxide (DMSO; 1%, v/v). Alkanes were added to the buffer using alkane stock solutions in DMSO. The reaction was initiated by addition of NADPH (200 µM), and the oxidation of NADPH was monitored at 340 nm [30]. The alkane substrate used was hexadecane.

2.6 Lipase assay

The lipase activity assay was conducted based on the spectrophotometric method described by Schultz et al., [31] with some modifications. The stoichiometric release of *p*-nitrophenol (p-NP) was measured from cleavage of *p*-nitrophenyl palmitate (*p*-NPP). *p*-NPP stock solution at concentration 100 mM was prepared in acetone and 30 µl was added to 2.82 mL of measuring buffer (0.1 M sodium phosphate, 10% v/v acetone, 4% v/w Triton X-100, 0.2% w/v gum arabic, pH 8.0). The prepared solution was incubated for 5 minutes in 60˚C water bath. Subsequently, it was cooled to 29˚C, added to a pre-warmed cuvette (29˚C), containing 150 µl of the lipase solution and placed into the temperature controlled spectrophotometer (Spectrophotometer CARY 300 UV-VIS). No mixing and no agitation were carried out. The measurements were conducted at 410 nm.

2.7 Preparation of the chitosan nanoparticles

Chitosan nanoparticles (CSNPs) were generated based on the ionotropic gelation technique, which exploits the electrostatic interaction between cations (amine group of chitosan) and a polyanion (TPP) [26].

Firstly, chitosan (CS) at a concentration of 2.5 mg/mL was dissolved in 2% acetic acid solution, and the pH was adjusted to 5.5 using 0.5 M NaOH. CS solution was constantly stirred for 1 h, with the speed ranging between 200 and 300 rpm. TPP

stock solution was prepared by dissolving TPP in deionized water to obtain its final concentration at 0.25 mg/mL. Subsequently, CS and TPP solutions were filtered via 0.45 μm membrane. A mixture of intracellular and extracellular enzymes of 10 mg/mL concentration (1:1 w/w) was added to chitosan solution and stirred for 15 minutes at ambient temperature. Later, TPP solution was added dropwise to enzyme-chitosan (ENZ-CS) solution, with different ratios (1:1 to 7:1). All the suspensions were stirred for 1 hour at 250 rpm. Afterward, 0.03% (v/v) of glutaraldehyde was added to all solutions and stirred for an extra hour at the ambient temperature. Finally, the suspensions were ultracentrifuged at 47,815 $x\ g$ for 2 h at 4 °C. The supernatant was separated and used to estimate the entrapment efficiency by measuring the unbound proteins. The pellet containing nanoparticles (NPs) was suspended in deionized water and used for further analysis.

2.8 Encapsulation efficiency

As mentioned earlier, the encapsulation efficiency (*EE*) was established by measuring the concentration of free enzyme in the supernatant, separated after ultracentrifugation. *EE* was calculated using the Equation (1):

Eq.(1) $$EE = \frac{Total\ enzyme\ activity\ used\ in\ formulation - activity\ of\ the\ free\ enzyme}{Total\ enzyme\ activity\ used\ in\ formulation} * 100$$

2.9 Characterization of enzyme-loaded chitosan nanoparticles: Particle size and zeta potential

The dynamic light scattering technique (25˚C, detection angle 90˚) was used to determine the particle size, size distribution (polydispersity index (PDI)) and zeta

potential of nanoparticles. All measurements were performed using Zetasizer (Malvern Instruments, US). The average particle size was approximated as the z-average diameter. The width of the distribution was defined as the PDI.

All measurements were performed in triplicate, and the results were reported as **a** mean ± standard deviation.

2.10 Fourier Transform Infrared Spectroscopy

The characteristic of the bonding between generated nanoparticles with encapsulated enzymes was analyzed by Fourier Transform Infrared Spectroscopy (FTIR) in transmission mode (Cary 670 FTIR Spectrometer). This technique helps to identify possible functional groups, which are responsible for nanoparticles stabilization. Spectra were performed at resolution 4 cm^{-1}, in the range of 4000-400 cm^{-1} with 100 scans.

2.11 Morphological observations

The morphology and size of the generated nanoparticles were investigated using scanning electron microscopy (SEM) (Carl ZeissEVO®50). The SEM samples were prepared by placing small drops of the diluted solution of nanoparticles on the aluminum foil and then dried at room temperature. The foil was fixed on the SEM instrument and coated with gold metal using a sputter coater.

2.12 In vitro enzyme release study

Encapsulated crude enzyme release from the nanoparticles complex was performed in two solutions: double distilled water (DDW) (pH 7) and phosphate buffer saline (PBS) solution (pH 7.4). Enzyme-loaded CS nanoparticles were suspended in each of these solutions. Later, they were incubated at ambient temperature. At specific time points, the samples of nanoparticles were collected

and centrifuged for 30 minutes, 25,000 x g, 4 ˚C. The supernatant was separated to measure the free alkane hydroxylase and lipase activities.

2.13. Stability of the free and immobilized enzymes

Double distilled water was used for measuring the stability of the free and immobilized alkane hydroxylase and lipase. Solutions of the immobilized and free enzyme were slowly homogenized and incubated at room temperature to measure the stability of both enzymes in time. Samples were drawn at 1, 5, 10, 15, 25 and 30 days for the determination of relative activity of enzymes.

2.14. Statistical analyses

Data in this study was summarized as the mean ± standard error (SD). Release profiles of enzymes from chitosan nanoparticles in both DDW and PBS were statistically evaluated using analysis of variance (ANOVA). Data from the three replicates of enzymes release were expressed as the mean ± standard deviation.

3. Results and discussion

3.1 Optimization of ENZ-CS and TPP mass ratio

Enzyme-loaded Chitosan nanoparticles (ENZ-loaded CSNPs) containing embedded alkane hydroxylase and lipase were prepared by ionotropic gelation technique.[32]. Based on the electrostatic interaction between the positively charged amino group of CS and oppositely charged phosphate of TPP. This technique was slightly modified by including glutaraldehyde at the end of the reaction, where the Schiff base reaction led to the higher stability of the nanoparticles by polymer crosslinking.

The choice of adding TPP into the protein-CS solution rather than adding TPP into CS solution was based on a previous study of Bahreini et al., [27] on enzyme encapsulation. In this study, both methods were tested and resulted in higher entrapment efficiency when adding TPP prior to mixing enzyme with chitosan, but no significant differences were observed in the particle size and zeta potential. This observation can be explained by possible interactions of the enzyme molecules with CS polymer before the addition of the cross-linker [27].

CS-TPP mass ratio was stated as a key parameter that influences the TPP and ENZ-CS cross-linking efficacy for nanoparticles formation. In fact, Jonassen et al., 2012 and Koukarass et al., 2012 [33,34] have reported that the long-term physical stability of chitosan nanoparticles cross-linked with TPP is affected by the ionic strength, the chitosan concentration, and the chitosan/TPP ratio employed in the particle preparation. Thus, an optimization study of ENZ-CS/TPP ratio was carried out to obtain the higher encapsulation efficiency. In fact, the nanoparticles formation started spontaneously after adding TPP to the ENZ-CS solution; the rapidity of their reaction is due to the molecular linkage between the positively charged chitosan amino groups and oppositely charged TPP phosphate ions [35].

Thus, chitosan mixed with the crude enzyme and TPP mass ratio varied from 1:1 to 7:1 as given in Table 1.

The ENZ-CS/TPP ratio of 5:1 showed the highest alkane hydroxylase and lipase encapsulation with 58.3% for alkane hydroxylase and 67.1% for lipase. Moreover, the calculation of the specific activity of the encapsulated alkane hydroxylase and lipase confirmed the results with best encapsulation shown for the ratio 5:1 with

3.9 U/µg and 11.7 U/ug, respectively. The ratio 4:1 for the encapsulated alkane hydroxylase showed the same specific activity as the ratio 5:1 (3.9 U/µg). Further decrease in ENZ-CS/TPP ratio led to the aggregation of the particles and high reaction response rate. The higher the volume of TPP, the more turbid the solution became, indicating a shift to higher particle size [34]. Comparable results were found by Zhang et al., [36] who reported an optimum ratio of 5:1 resulting in the finest particle size, while Koukaras et al., [37] reported an optimum of 4:1.

Low ratios of 1:1 to 4:1 showed the appearance of high turbidity, due to the increased aggregation of nanoparticles and a shift to higher particle size. Jonassem et al., [38] confirmed the high turbidity when switching from a particle size of 720.4 nm to 1032 nm. Thus, these ratios were discarded. Nanoparticle aggregation takes place under some conditions, such as inappropriate homogenization speed, or higher concentration of cross-linker [39].

Furthermore, with the decrease in ENZ-CS/TPP mass ratio from 7:1 to 1:1, zeta potential increased from +21.1 to +36.7 mV, respectively, and pH of the resulting formulation ranged from 5.64 to 5.89. The diminution of zeta potential occurred due to the reduction of chitosan -NH_3^+ groups caused by further enzyme loading [27]. The crude enzyme was used for nanoparticle loading, thus the enzyme solution contained a mixture of proteins, which possess various physicochemical features (i.e. pI, structure). Hence, during cross-linking, the negatively charged groups on protein surface was neutralized by positively charged amine groups of chitosan as shown in Fig. 1 (protein A situation). Additionally, -$NH3^+$ groups on the enzyme surface might be counteracted by polyanionic TPP molecules (Fig. 1, protein B situation). This results in compression of the proteins inside the

particles and on their surface. The nanoparticles, as potential protein carriers, must be able to ionically hold the active molecules. Thus, the sufficient zeta potential value is essential for these nanoparticles. Particles with zeta potential between 20 – 25 mV exhibit relative stability [40]. On the other hand, alkane hydroxylase encapsulation increased from 0% to 58.7% with decreasing ENZ-CS/TPP ratio from 7:1–5:1 and increased lipase encapsulation from 1.5% to 67.1% for the same ratios. And even further decrease in ENZ-CS/TPP ratio resulted in no significant change in the encapsulation of ENZ and in fact increased the particle size.

The immobilization of lipase on SnO_2 hollow nanotubes investigated by Anwar et al., [15] showed an efficiency of 89%. Also, lipase nanohybrid synthesized using cobalt chloride studied by Kumar et al., [21] exhibited 181% higher activity compared to the free lipase. Moreover, Gill et al., [41] reported 59% and 70% of laccase encapsulation efficiency when using alginate and silica incorporated into alginate, respectively as supports. Patel et al., [42] demonstrated the improvement of the immobilization efficiency of laccase, from 83.5% to 90.2%, when using glutaraldehyde as a cross linker.

3.2 Fourier Transform InfraRed spectrometry study

The FTIR spectra for the enzyme (A), CS (B), CS blank NPs (C), and ENZ-loaded CSNPs (D) are shown in Fig. 2. The peaks at 2,967 cm^{-1} in the enzyme spectrum (A) and at 3,292 cm^{-1} in the CS spectrum (B) relate to the stretching of O-H and N-H bonds. In the CSNPs spectrum (C), the peak at 3,292 cm^{-1} becomes much more intense; pointing out the $–NH_3^+$ interactions with negatively charged TPP. A corresponding peak in the ENZ-loaded CSNPs (D) at 2840 cm^{-1} becomes

wider; this effect is attributable to the participation of the enzyme in hydrogen bonding and -NH group interactions [43].

In CS blank NPs, the 1,562 cm^{-1} peaks of $-NH_2$ bending vibration shifts to 1,630 cm^{-1} and became sharper. This can be a hydrogen bond and amide bond linkage in chitosan with phosphoric groups of TPP; inter- and intra-molecular interactions are enhanced in CS blank NPs [44]. A shift from 1,017 cm^{-1} to a peak at 1,051 cm^{-1} in CS blank NPs to a sharper peak at 1010 cm^{-1} in ENZ-loaded CS NPs corresponds to the stretching vibration of the P =O groups.

Two high-intensity peaks at 1,550 cm^{-1} (amide I bending) and 1,400 cm^{-1} (amide II bending) in ENZ-loaded CSNPs correspond to the small intensity peaks at 1,393 and 1,247 cm^{-1} in the enzyme spectra and to the peaks at 1,562 cm^{-1} and 1,370 cm^{-1} in CS spectra. These results prove successful loading of the enzyme in CSNPs and also indicates some interactions between CS with TPP and the crude enzyme [45].

3.3 Morphology study

Fig. 3 shows the morphological characteristics of CSNPs (A), ENZ-loaded CSNPs (B) and the supernatant of chitosan solution containing the non-encapsulated enzymes (C). From the SEM images, it can be noticed that CSNPs (A) have a spherical morphology with some irregularities on the surface (white needle-like structures). ENZ-loaded CSNPs (B) are also spherical, however, their surface smoothens. In both cases, the particles aggregate, which may have been generated during drying step [46]. As for the morphology of the supernatant (C), it shows the same rough spherical morphology as Fig. 3 (A) with non-regular spheres in between which are obviously the enzymes. Furthermore, the

nanometric size estimated through DLS (Dynamic Light Scattering) of the enzymatic preparation is correlated to the average particle size revealed by SEM which is ~ 430 nm.

In Fig. 3 (A), a fairly uniform particle size distribution (the average size is ~ 203 nm) and the smooth border around the CS blank NPs was noticed. In Fig. 3 (B), ENZ-loaded CSNPs showed an asymmetrical, but smoothened spherical shape that is obviously induced by the presence of the enzyme. It can also be noted that the size of the core of the ENZ-loaded CSNPs (the average size is ~ 430 nm) is approximately 2-fold larger than the particle size of CSNPs. Consequently, it could be assumed that the significantly increased size of the ENZ-loaded CSNPs estimated through SEM and also through DLS is due to the enzymes that coated the surface. The protein effect on the nanoparticle size and their shape due to the chitosan-protein ionic interaction has been previously reported by Rampino et al., [35]. Furthermore, in another study of Sadighi et Faramarzi, [47], it was discovered that laccase immobilization on the surface of CSNPs induced a change in the nanoparticles morphology. Unloaded chitosan nanoparticles were reported as polyhedron shaped, however, due to the bovine serum albumin incorporation in CS, the particles became spherical and smooth surfaced which is comparable to this study [48].

3.4 In vitro alkane hydroxylase and lipase release study

Fig. 4 shows alkane hydroxylase and lipase release profiles from the ENZ-loaded CSNPs in two different solutions (DDW and PBS) that have approximately the same pH as the ones that can be found in petroleum contaminated water and soil. Alkane hydroxylase loaded CSNPs incubated in DDW (pH 7) (Fig. 4 (A)) showed

no release until the first 24 h. A release of 3.2% was shown starting from 48h, 36.7% release for one week, and 74.3% release for 17 days. Alkane hydroxylase release in PBS was negligible after 3 hours (1.2%), 33.4% release during 24 h, 45.2% release during 48 h and 80.3% release after 8 days only. Further increase in release time resulted in no significant change (p>0.05).

Lipase loaded CSNPs incubated in DDW (pH 7) (Fig. 4 (B)) showed no release until the first 24 hours with 4.8% release. A 41% release was shown for one week, and 79.3% release during 17 days. Alkane hydroxylase release in PBS with started after 2 hours (1.3%). 52.8% release was shown during 24 h, 60.9% release during 48 h, and 88.1% release after 8 days only. After 8 days no significant change in release was shown (p>0.05). Several factors influence the burst release of enzyme from CSNPs such as pH of the solution and ionic strength of PBS [27]. Firstly, pH is a crucial parameter in the stability and release of the protein from the CS matrix. The pK_a value of CS is 6.5, thus the $-NH_2$ groups of CS are protonated at lower pH ($-NH_3^+$). However, when pH is higher than its pK_a the amine group is converted to non-ionized state. This results in the reduction of the cross-linking area with negatively charged TPP molecules [49,50]. Moreover, with the increase of pH, the increased permeation of water occurs [51]. Hence, at neutral pH of this study, the CSNPs may undergo elongation due to the diffusion, which leads to an extension of particle size and release of protein.

The CS-TPP interaction may also be influenced by the ionic strength of the media. The presence of NaCl in PBS buffer at lower or moderate concentrations resulted in enhancement of the CSNPs swelling, which attenuated the CS-TPP interaction and disintegrated NPs [52]. Hence, the CSNPs increase their volume

by swelling and then their structure collapses which lead to the biomolecule release. This may be the reason for the faster release of enzymes in PBS solution than in DDW solution.

3.5 Kinetics of the release study

The ENZ release from CSNPs was fitted to the most common kinetic models to determine the release characteristics. The parameters of the release study for various mathematical models are presented in Table 2. Based on the higher linearity of the plots (R^2>0.97), the best model that fits the alkane hydroxylase release in DDW is a zero-order kinetic model. This results in their slow release from CS matrix, however, the release does not depend on the concentration of the initial enzyme [53,54]. This result can be confirmed by diffusional release exponent value (n~1). In the case of the release of alkane hydroxylase in PBS, it followed Higuchi kinetic model (R^2>0.93) [55]. The results suggested that the discharge of the biomolecule is based on the Fick's diffusion law [53]. Hence, the release of the biomolecule depends on the diffusion rate throughout the CS matrix in both cases.

The lipase release in DDW and PBS followed the Korsmeyer-Peppas model [56]. In DDW, the diffusional release exponent value was between 0.5 and 1, thus the lipase discharge is non-Fickian (anomalous transport). However, in PBS sthe *n* value decreased (n<0.5), which suggests that lipase release depended on the diffusion (Fick's first law).

As can be observed, the kinetic model depends on the media in which CS-ENZ particles are present. As discussed earlier, PBS has higher ionic strength than DDW, which results in CS particles swelling and faster release than in solutions

with low ionic strength [57]. Hence, the release kinetic model changes with the alteration of the media. Furthermore, alkane hydroxylase and lipase do not follow the same release model. This suggests that the interaction between the media and CSNPs differs due to the variable structure or overall charge (pI).

3.6 In vitro half-life of free and immobilized enzymes

In general, the free enzymes are not stable and rapidly lose their activity [58] . Gradual and faster depletion of catalytic activity with time and recovery problems after reactions limited the applications of free enzymes. Thus, different immobilization technologies were investigated to overcome these barriers [60]. The higher half-life of the enzyme reflects their stability and is one of the main standards to estimate the performance of enzyme. Consequently, immobilized enzymes are considered more performant compared to the free enzyme. Fig. 5 (A) and Fig. 5 (B) exhibit the profiles feature of the free and immobilized alkane hydroxylase and lipase. Both enzymes were kept at room temperature for up to 30 days and their activities were determined periodically to evaluate their half-life. The results demonstrated that both alkane hydroxylase-loaded CSNPS and lipase-loaded CSNPs had longer half-life than the free enzymes in a one month study period. Moreover, the deactivation constant k_d is lower for both immobilized enzymes than that for the free enzymes (Table 3) which was also reported in previous studies [18].

During the first 5 days of incubation, free alkane hydroxylase lost 43% of its activity while immobilized alkane hydroxylase lost only 21% of the activity. Lipase free enzyme lost 58% of activity after the first 5 days while the immobilized form of lipase maintained 72% of its activity. After 30 days, free

alkane hydroxylase and also free lipase lost 100% of their catalytic activity, while immobilized alkane hydroxylase and lipase maintained 17% and 13% of the initial activity, respectively.

Same results were found for oxidoreductase type of enzymes, such as laccase immobilized on polymeric nanofibers with 60% residual activity of the immobilized enzyme and almost no activity for the free laccase after 10 days [61]. Chiou et Wu, [62] observed that the activity of lipase decreased more than 50% in 5 days, while the lipase immobilized to wet chitosan beads did not show any activity reduction up to 30 days at 25 °C [62].

4. Conclusion

A successful nano-encapsulation of alkane hydroxylase and lipase produced from the hydrocarbonoclastic bacteria *Alcanivorax borkumensis* in chitosan polymer has been achieved with homogeneously nano-sized particle formation. To the best of our knowledge, this is the first report about immobilization of enzymes produced from *Alkanivorax borkumensis* and also first report on nano-encapsulation of lipase and alkane hydroxylase using chitosan. Different enzyme-chitosan/tripolyphosphate ratios were studied and (5:1) was maintained for the best entrapment efficiency for both alkane hydroxylase and lipase with a particle size and a zeta potential of 473 nm and +21.8, respectively. Entrapment efficiency for alkane hydroxylase loaded chitosan nano-particles CSNPs and lipase loaded chitosan nanoparticles was 58.3% and 67.1%, respectively. Interestingly, the half-life catalytic activity of the immobilized enzymes was very important, even after 30 days compared to the free enzymes. This in vitro study would provide an

interesting impetus for the future in vivo study of the formulation of crude enzymes from *A. borkumensis* for the degradation of petroleum hydrocarbons in the field.

Acknowledgement

The authors are sincerely thankful to the Natural Sciences and Engineering Research Council of Canada (Discovery Grant 355254, CRD Grant and Strategic Grant 447075) and Techno-Rem Inc. for financial support. We also thank Anne-Marie Lapointe for her valuable contribution to this work. The views or opinions expressed in this article are those of the authors.

References

[1] M.V. Faustorilla, Z. Chen, R. Dharmarajan, R. Naidu, Determination of Total Petroleum Hydrocarbons in Australian Groundwater Through the Improvised Gas Chromatography–Flame Ionization Detection Technique, J. Chromatogr. Sci. (2017) 1–9.

[2] I.B. Ivshina, M.S. Kuyukina, A.V. Krivoruchko, A.A. Elkin, S.O. Makarov, C.J. Cunningham, T.A. Peshkur, R.M. Atlas, J.C. Philp, Oil spill problems and sustainable response strategies through new technologies, Environ. Sci. Process. Impacts. 17 (2015) 1201–1219.

[3] R. Kumar, A.J. Das, A.A. Juwarkar, Reclamation of petrol oil contaminated soil by rhamnolipids producing PGPR strains for growing Withania somnifera a medicinal shrub, World J. Microbiol. Biotechnol. 31 (2015) 307–313.

[4] N. Kumari, A. Vashishtha, P. Saini, E. Menghani, Isolation, identification and characterization of oil degrading bacteria isolated from the

contaminated sites of Barmer, Rajasthan, Int J Biotechnol Bioeng Res. 4 (2013) 429–436.
[5] N. Das, P. Chandran, Microbial degradation of petroleum hydrocarbon contaminants: an overview, Biotechnol. Res. Int. 2011 (2010). http://www.hindawi.com/journals/btri/2011/941810/abs/ (accessed October 5, 2016).
[6] M.M. Yakimov, K.N. Timmis, P.N. Golyshin, Obligate oil-degrading marine bacteria, Curr. Opin. Biotechnol. 18 (2007) 257–266.
[7] L. Wang, W. Wang, Q. Lai, Z. Shao, Gene diversity of CYP153A and AlkB alkane hydroxylases in oil-degrading bacteria isolated from the Atlantic Ocean, Environ. Microbiol. 12 (2010) 1230–1242.
[8] W. Wang, L. Wang, Z. Shao, Diversity and abundance of oil-degrading bacteria and alkane hydroxylase (alkB) genes in the subtropical seawater of Xiamen Island, Microb. Ecol. 60 (2010) 429–439.
[9] M. Bookstaver, M.P. Godfrin, A. Bose, A. Tripathi, An insight into the growth of Alcanivorax borkumensis under different inoculation conditions, J. Pet. Sci. Eng. 129 (2015) 153–158. doi:10.1016/j.petrol.2015.02.038.
[10] M. Hassanshahian, G. Emtiazi, G. Caruso, S. Cappello, Bioremediation (bioaugmentation/biostimulation) trials of oil polluted seawater: a mesocosm simulation study, Mar. Environ. Res. 95 (2014) 28–38.
[11] D.J. Naether, S. Slawtschew, S. Stasik, M. Engel, M. Olzog, L.Y. Wick, K.N. Timmis, H.J. Heipieper, Adaptation of the Hydrocarbonoclastic Bacterium Alcanivorax borkumensis SK2 to Alkanes and Toxic Organic Compounds: a Physiological and Transcriptomic Approach, Appl. Environ. Microbiol. 79 (2013) 4282–4293. doi:10.1128/AEM.00694-13.
[12] S.-H. Naing, S. Parvez, M. Pender-Cudlip, J.T. Groves, R.N. Austin, Substrate specificity and reaction mechanism of purified alkane hydroxylase from the hydrocarbonoclastic bacterium Alcanivorax borkumensis (AbAlkB), J. Inorg. Biochem. 121 (2013) 46–52.
[13] S. Schneiker, V.A.M. dos Santos, D. Bartels, T. Bekel, M. Brecht, J. Buhrmester, T.N. Chernikova, R. Denaro, M. Ferrer, C. Gertler, A. Goesmann, O.V. Golyshina, F. Kaminski, A.N. Khachane, S. Lang, B. Linke, A.C. McHardy, F. Meyer, T. Nechitaylo, A. Pühler, D. Regenhardt, O. Rupp, J.S. Sabirova, W. Selbitschka, M.M. Yakimov, K.N. Timmis, F.-J. Vorhölter, S. Weidner, O. Kaiser, P.N. Golyshin, Genome sequence of the ubiquitous hydrocarbon-degrading marine bacterium Alcanivorax borkumensis, Nat. Biotechnol. 24 (2006) 997–1004. doi:10.1038/nbt1232.
[14] G.A.-E. Mahmoud, M.M. Koutb, F.M. Morsy, M.M. Bagy, Characterization of lipase enzyme produced by hydrocarbons utilizing fungus Aspergillus terreus, Eur. J. Biol. Res. 5 (2015) 70–77.
[15] M.Z. Anwar, D.J. Kim, A. Kumar, S.K. Patel, S. Otari, P. Mardina, J.-H. Jeong, J.-H. Sohn, J.H. Kim, J.T. Park, SnO 2 hollow nanotubes: a novel and efficient support matrix for enzyme immobilization, Sci. Rep. 7 (2017) 15333.

[16] M. Naghdi, M. Taheran, S.K. Brar, A. Kermanshahi-pour, M. Verma, R.Y. Surampalli, Immobilized laccase on oxygen functionalized nanobiochars through mineral acids treatment for removal of carbamazepine, Sci. Total Environ. 584 (2017) 393–401.
[17] S.K. Patel, M.Z. Anwar, A. Kumar, S.V. Otari, R.T. Pagolu, S.-Y. Kim, I.-W. Kim, J.-K. Lee, Fe 2 O 3 yolk-shell particle-based laccase biosensor for efficient detection of 2, 6-dimethoxyphenol, Biochem. Eng. J. (2017).
[18] S.K. Patel, S.V. Otari, Y.C. Kang, J.-K. Lee, Protein–inorganic hybrid system for efficient his-tagged enzymes immobilization and its application in L-xylulose production, RSC Adv. 7 (2017) 3488–3494.
[19] S.K. Patel, S.H. Choi, Y.C. Kang, J.-K. Lee, Eco-friendly composite of Fe3O4-reduced graphene oxide particles for efficient enzyme immobilization, ACS Appl. Mater. Interfaces. 9 (2017) 2213–2222.
[20] M. Taheran, M. Naghdi, S.K. Brar, E.J. Knystautas, M. Verma, R.Y. Surampalli, Degradation of chlortetracycline using immobilized laccase on Polyacrylonitrile-biochar composite nanofibrous membrane, Sci. Total Environ. 605 (2017) 315–321.
[21] A. Kumar, I.-W. Kim, S.K. Patel, J.-K. Lee, Synthesis of Protein-Inorganic Nanohybrids with Improved Catalytic Properties Using Co 3 (PO 4) 2, Indian J. Microbiol. 58 (2018) 100–104.
[22] S.K. Patel, S.V. Otari, J. Li, D.R. Kim, S.C. Kim, B.-K. Cho, V.C. Kalia, Y.C. Kang, J.-K. Lee, Synthesis of cross-linked protein-metal hybrid nanoflowers and its application in repeated batch decolorization of synthetic dyes, J. Hazard. Mater. (2018).
[23] A. Dzionek, D. Wojcieszyńska, U. Guzik, Natural carriers in bioremediation: A review, Electron. J. Biotechnol. 23 (2016) 28–36.
[24] S.K. Patel, R.K. Singh, A. Kumar, J.-H. Jeong, S.H. Jeong, V.C. Kalia, I.-W. Kim, J.-K. Lee, Biological methanol production by immobilized Methylocella tundrae using simulated biohythane as a feed, Bioresour. Technol. 241 (2017) 922–927.
[25] S.K. Patel, S. Kondaveeti, S.V. Otari, R.T. Pagolu, S.H. Jeong, S.C. Kim, B.-K. Cho, Y.C. Kang, J.-K. Lee, Repeated batch methanol production from a simulated biogas mixture using immobilized Methylocystis bryophila, Energy. (2017).
[26] R. Pulicharla, C. Marques, R.K. Das, T. Rouissi, S.K. Brar, Encapsulation and release studies of strawberry polyphenols in biodegradable chitosan nanoformulation, Int. J. Biol. Macromol. 88 (2016) 171–178.
[27] E. Bahreini, K. Aghaiypour, R. Abbasalipourkabir, A.R. Mokarram, M.T. Goodarzi, M. Saidijam, Preparation and nanoencapsulation of l-asparaginase II in chitosan-tripolyphosphate nanoparticles and in vitro release study, Nanoscale Res. Lett. 9 (2014) 340.
[28] M.M. Yakimov, P.N. Golyshin, S. Lang, E.R. Moore, W.-R. Abraham, H. Lünsdorf, K.N. Timmis, Alcanivorax borkumensis gen. nov., sp. nov., a new, hydrocarbon-degrading and surfactant-producing marine bacterium, Int. J. Syst. Evol. Microbiol. 48 (1998) 339–348.

[29] M.M. Bradford, A rapid and sensitive method for the quantitation of microgram quantities of protein utilizing the principle of protein-dye binding, Anal. Biochem. 72 (1976) 248–254.
[30] A. Glieder, E.T. Farinas, F.H. Arnold, Laboratory evolution of a soluble, self-sufficient, highly active alkane hydroxylase, Nat. Biotechnol. 20 (2002) 1135–1139. doi:10.1038/nbt744.
[31] N. Schultz, T.J. Hobley, C. Syldatk, Spectrophotometric assay for online measurement of the activity of lipase immobilised on micro-magnetic particles, Biotechnol. Lett. 29 (2007) 365–371.
[32] P. Calvo, C. Remuñan-López, J.L. Vila-Jato, M.J. Alonso, Chitosan and chitosan/ethylene oxide-propylene oxide block copolymer nanoparticles as novel carriers for proteins and vaccines, Pharm. Res. 14 (1997) 1431–1436.
[33] E.N. Koukaras, S.A. Papadimitriou, D.N. Bikiaris, G.E. Froudakis, Insight on the formation of chitosan nanoparticles through ionotropic gelation with tripolyphosphate, Mol. Pharm. 9 (2012) 2856–2862.
[34] H. Jonassen, A.-L. Kjøniksen, M. Hiorth, Stability of chitosan nanoparticles cross-linked with tripolyphosphate, Biomacromolecules. 13 (2012) 3747–3756.
[35] A. Rampino, M. Borgogna, P. Blasi, B. Bellich, A. Cesàro, Chitosan nanoparticles: preparation, size evolution and stability, Int. J. Pharm. 455 (2013) 219–228.
[36] H. Zhang, M. Oh, C. Allen, E. Kumacheva, Monodisperse chitosan nanoparticles for mucosal drug delivery, Biomacromolecules. 5 (2004) 2461–2468.
[37] E.N. Koukaras, S.A. Papadimitriou, D.N. Bikiaris, G.E. Froudakis, Insight on the formation of chitosan nanoparticles through ionotropic gelation with tripolyphosphate, Mol. Pharm. 9 (2012) 2856–2862.
[38] H. Jonassen, A.-L. Kjøniksen, M. Hiorth, Effects of ionic strength on the size and compactness of chitosan nanoparticles, Colloid Polym. Sci. 290 (2012) 919–929.
[39] Q. Gan, T. Wang, Chitosan nanoparticle as protein delivery carrier—systematic examination of fabrication conditions for efficient loading and release, Colloids Surf. B Biointerfaces. 59 (2007) 24–34.
[40] D.-W. Lee, K. Powers, R. Baney, Physicochemical properties and blood compatibility of acylated chitosan nanoparticles, Carbohydr. Polym. 58 (2004) 371–377.
[41] J. Gill, V. Orsat, S. Kermasha, Optimization of encapsulation of a microbial laccase enzymatic extract using selected matrices, Process Biochem. (2017).
[42] S.K. Patel, S.H. Choi, Y.C. Kang, J.-K. Lee, Large-scale aerosol-assisted synthesis of biofriendly Fe 2 O 3 yolk–shell particles: a promising support for enzyme immobilization, Nanoscale. 8 (2016) 6728–6738.
[43] Y. Wu, W. Yang, C. Wang, J. Hu, S. Fu, Chitosan nanoparticles as a novel delivery system for ammonium glycyrrhizinate, Int. J. Pharm. 295 (2005) 235–245.

[44] J.Z. Knaul, S.M. Hudson, K.A. Creber, Improved mechanical properties of chitosan fibers, J. Appl. Polym. Sci. 72 (1999) 1721–1732.
[45] Y. Xu, Y. Du, Effect of molecular structure of chitosan on protein delivery properties of chitosan nanoparticles, Int. J. Pharm. 250 (2003) 215–226.
[46] Y. Luo, B. Zhang, W.-H. Cheng, Q. Wang, Preparation, characterization and evaluation of selenite-loaded chitosan/TPP nanoparticles with or without zein coating, Carbohydr. Polym. 82 (2010) 942–951.
[47] A. Sadighi, M.A. Faramarzi, Congo red decolorization by immobilized laccase through chitosan nanoparticles on the glass beads, J. Taiwan Inst. Chem. Eng. 44 (2013) 156–162.
[48] Q. Gan, T. Wang, C. Cochrane, P. McCarron, Modulation of surface charge, particle size and morphological properties of chitosan–TPP nanoparticles intended for gene delivery, Colloids Surf. B Biointerfaces. 44 (2005) 65–73.
[49] H.-Q. Mao, K. Roy, V.L. Troung-Le, K.A. Janes, K.Y. Lin, Y. Wang, J.T. August, K.W. Leong, Chitosan-DNA nanoparticles as gene carriers: synthesis, characterization and transfection efficiency, J. Controlled Release. 70 (2001) 399–421.
[50] X.Z. Shu, K.J. Zhu, A novel approach to prepare tripolyphosphate/chitosan complex beads for controlled release drug delivery, Int. J. Pharm. 201 (2000) 51–58.
[51] W. Ajun, S. Yan, G. Li, L. Huili, Preparation of aspirin and probucol in combination loaded chitosan nanoparticles and in vitro release study, Carbohydr. Polym. 75 (2009) 566–574.
[52] T. López-León, E.L.S. Carvalho, B. Seijo, J.L. Ortega-Vinuesa, D. Bastos-González, Physicochemical characterization of chitosan nanoparticles: electrokinetic and stability behavior, J. Colloid Interface Sci. 283 (2005) 344–351.
[53] P. Costa, J.M.S. Lobo, Modeling and comparison of dissolution profiles, Eur. J. Pharm. Sci. 13 (2001) 123–133.
[54] M. Miastkowska, E. Sikora, J. Ogonowski, M. Zielina, A. \Ludzik, The kinetic study of isotretinoin release from nanoemulsion, Colloids Surf. Physicochem. Eng. Asp. 510 (2016) 63–68.
[55] T. Higuchi, Mechanism of sustained-action medication. Theoretical analysis of rate of release of solid drugs dispersed in solid matrices, J. Pharm. Sci. 52 (1963) 1145–1149.
[56] R.W. Korsmeyer, R. Gurny, E. Doelker, P. Buri, N.A. Peppas, Mechanisms of solute release from porous hydrophilic polymers, Int. J. Pharm. 15 (1983) 25–35.
[57] X.Z. Shu, K.J. Zhu, Controlled drug release properties of ionically cross-linked chitosan beads: the influence of anion structure, Int. J. Pharm. 233 (2002) 217–225.
[58] H. Zaak, E.-H. Siar, J.F. Kornecki, L. Fernandez-Lopez, S.G. Pedrero, J.J. Virgen-Ortíz, R. Fernandez-Lafuente, Effect of immobilization rate and enzyme crowding on enzyme stability under different conditions. The

case of lipase from Thermomyces lanuginosus immobilized on octyl agarose beads, Process Biochem. 56 (2017) 117–123.
[59] A.A. De Queiroz, E.D. Passos, S. De Brito Alves, G.S. Silva, O.Z. Higa, M. Vítolo, Alginate–poly (vinyl alcohol) core–shell microspheres for lipase immobilization, J. Appl. Polym. Sci. 102 (2006) 1553–1560.
[60] U. Guzik, K. Hupert-Kocurek, D. Wojcieszyńska, Immobilization as a strategy for improving enzyme properties-application to oxidoreductases, Molecules. 19 (2014) 8995–9018.
[61] R. Xu, Q. Zhou, F. Li, B. Zhang, Laccase immobilization on chitosan/poly (vinyl alcohol) composite nanofibrous membranes for 2, 4-dichlorophenol removal, Chem. Eng. J. 222 (2013) 321–329.
[62] S.-H. Chiou, W.-T. Wu, Immobilization of Candida rugosa lipase on chitosan with activation of the hydroxyl groups, Biomaterials. 25 (2004) 197–204. doi:10.1016/S0142-9612(03)00482-4.

Tables:

Table 1. Parameters for optimization of CS-TPP mass ratio.

Chitosan/Sodium tripolyphosphate ratio	Particle size (nm)	Zeta potential (mV)	PDI	pH of chitosan solution (SD ± 0.05)	pH of the formulation (SD ± 0.05)
1:1	720.4±8.2	+36.7±2.0	0.55±0.12	5.50	5.89
2:1	814.1±4.5	+34.2±3.0	0.56±0.08	5.50	5.66
3:1	1032±9.8	+31.5±4.0	0.50±0.06	5.50	5.67
4:1	999.4±6.6	+24.6±3.0	1.00±0.21	5.50	5.7
5:1	**473.6±7.3**	**+21.8±2.0**	**1.00±0.09**	**5.50**	**5.81**
6:1	433.6±4.5	+21.1±3.0	1.00±0.11	5.50	5.83
7:1	1104.0±8.7	+20.4±2.0	0.50±0.08	5.50	5.64

Chitosan/Sodium tripolyphosphate ratio	Free Alkane hydroxylase activity (U)	Alkane hydroxylase activity in the supernatant (U)	Specific activity of the encapsulated alkane hydroxylase (U/µg proteins)	% of encapsulation of alkane hydroxylase	Free lipase activity (U)	Lipase activity in the supernatant (U)	Specific activity of the encapsulated lipase (U/µg proteins)
1:1	115.6±2.1	58.9±1.1	1.9±0.1	49.0	254.4±1.4	140.2±2.4	3.9±0.1
2:1	154.1±1.3	83.7±0.8	2.5±0.1	45.7	310.3±2.7	163.0±3.7	5.3±0.2
3:1	173.6±2.9	86.74±1.2	2.9±0.3	50.0	405.3±5.8	208.1±4.6	6.6±0.2
4:1	185.0±2.0	79.2±0.7	3.9±0.4	57.2	411.7±5.0	187.0±3.5	8.5±0.6
5:1	**192.7±1.7**	**80.2±1.3**	**3.9±0.6**	**58.3**	**499.8±5.6**	**164.2±2.7**	**11.7±0.4**
6:1	198.2±2.4	179.7±1.8	0.5±0.04	9.3	507.7±6.5	459.4±8.5	1.5±0.1
7:1	202.4±1.8	204.1±1.5	0.0	0.0	515.0±7.3	507.3±6.6	0.2±0.03

Table 2. Kinetic model parameters fitting into the enzyme release study.

Model	Equation	Parameter	Alkane hydroxylase		Lipase	
			DDW	PBS	DDW	PBS
Zero order	$Q_t=Q_0+K_0t$	R^2	**0.979**	0.903	0.978	0.803
First order	$\ln Q_t=\ln Q_0+K_1t$	R^2	0.732	0.598	0.807	0.478
Higuchi	$Q_t=Q_0+K_Ht^{1/2}$	R^2	0.932	**0.983**	0.953	0.932
Korsmeyer-Peppas	$Q_t=Q_0+K_{KP}^n$	n R^2	0.993 0.977	0.561 0.976	0.895 **0.981**	0.434 **0.941**

Q_t- the activityof enzymes released in time t; Q_0- initial activity of enzymes; K_0- zero-order kinetic constant; K_1- first order kinetic constant; K_H- Higuchi kinetic constant, t- time

Table 3. Half-life of the free and immobilized enzymes.

	Free lipase	**Immobilized lipase**	**Free alkane hydroxylase**	**Immobilized alkane hydroxylase**
Half-life (day)	4.62	11.60	5.96	11.95
Deactivation constant k_d (day^{-1})	0.15	0.06	0.12	0.06

Figure captions:

Fig. 1. Hypothesis of the mechanism of immobilization of enzymes in chitosan nanoparticles.

Fig. 2. FTIR spectra of: (A) Crude enzyme, (B) Chitosan, (C) Non-loaded nanoparticles, and (D) Loaded nanoparticles.

Fig. 3. Scanning electron microscopy images of CSNPs (A), ENZ-loaded CSNPs (B) and non-encapsulated enzyme (D). Particles size shown in SEM is 203 nm for CSNPs and 430 nm for ENZ-loaded CSNPs.

Fig. 4. Alkane hydroxylase (A) and lipase (B) release profiles from the ENZ-loaded CSNPs in two different solutions: double distilled water and phosphate buffer saline.

Fig. 5. In vitro half-life of the free and immobilized alkane hydroxylase (A) and; lipase (B).

Fig.1. Hypothesis of the mechanism of immobilization of enzymes in chitosan nanoparticles

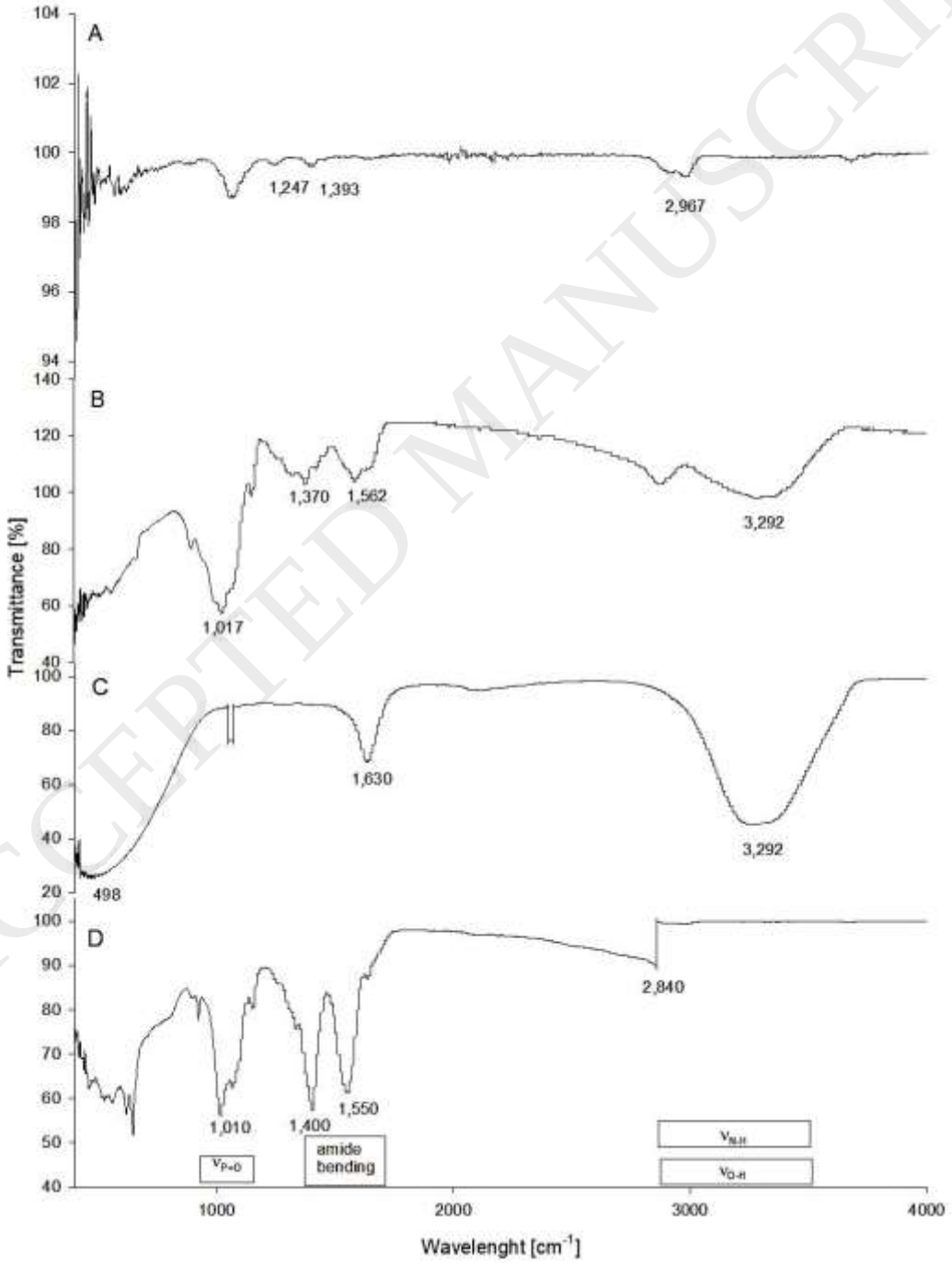

Fig. 2. FTIR spectra of: (A) Crude enzyme, (B) Chitosan, (C) Non-encapsulated enzyme, and (D) ENZ-loaded CSNPs

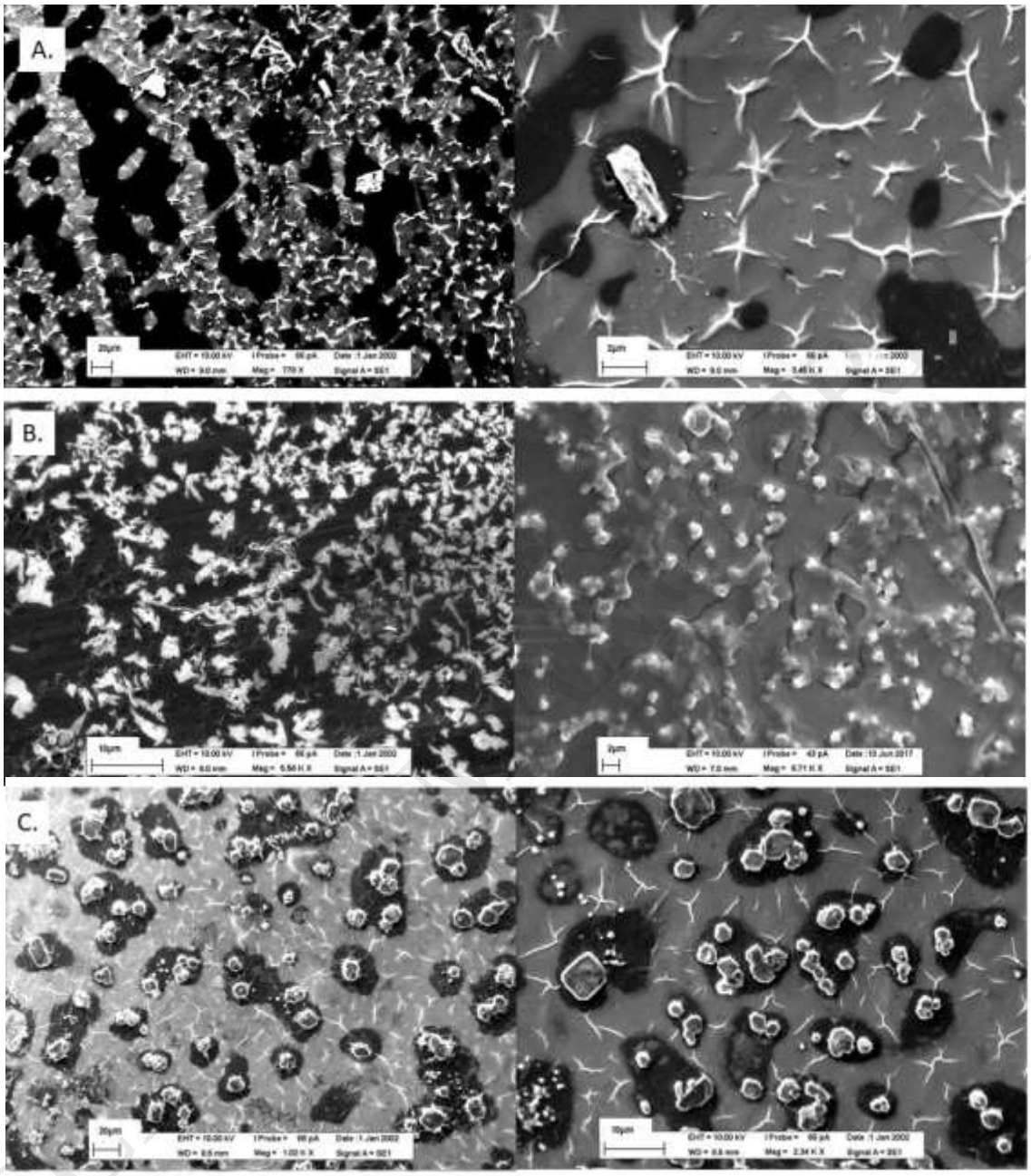

Fig. 3. Scanning electron microscopy images of: CSNPs (A), ENZ-loaded CSNPs (B) and; non-encapsulated enzyme (C). Particles size shown in SEM is 203 nm for CSNPs and 430 nm for ENZ-loaded CSNPs.

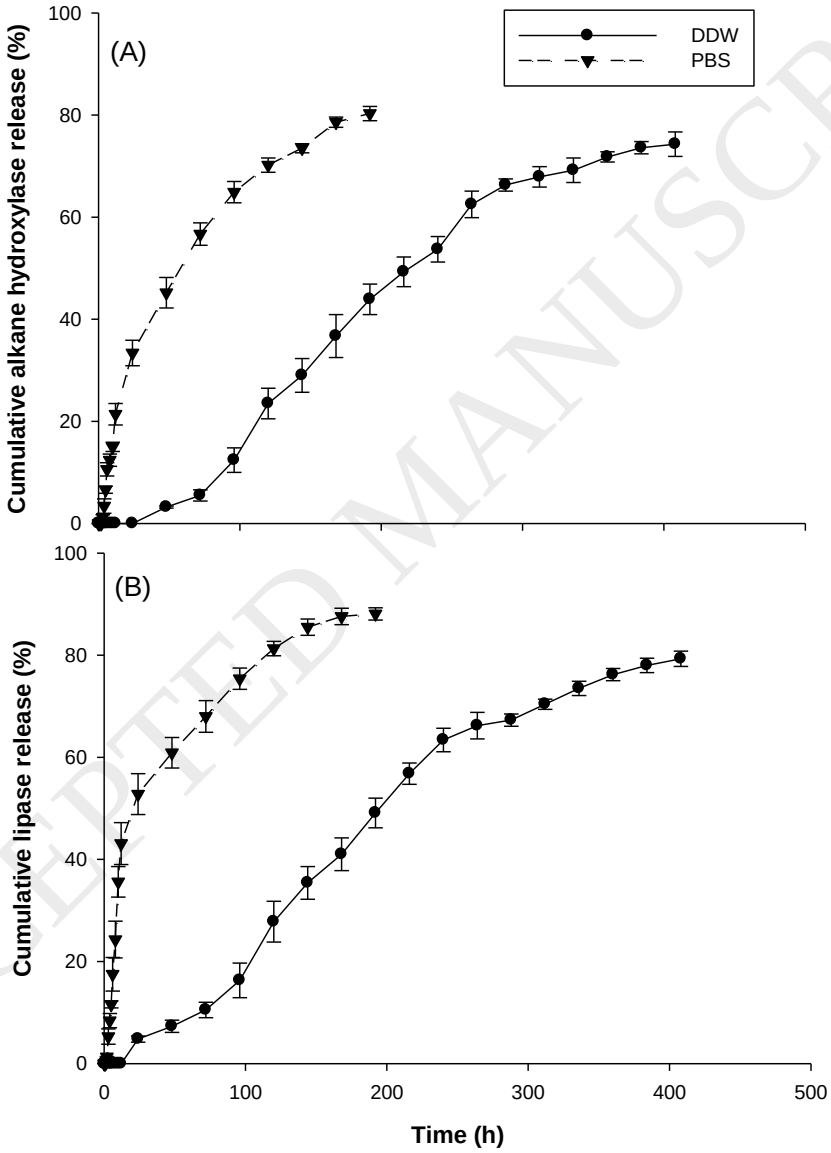

Fig. 4. Alkane hydroxylase (A); and lipase (B) release profiles from the ENZ-loaded CSNPs in two different solutions: double distilled water and phosphate buffer saline.

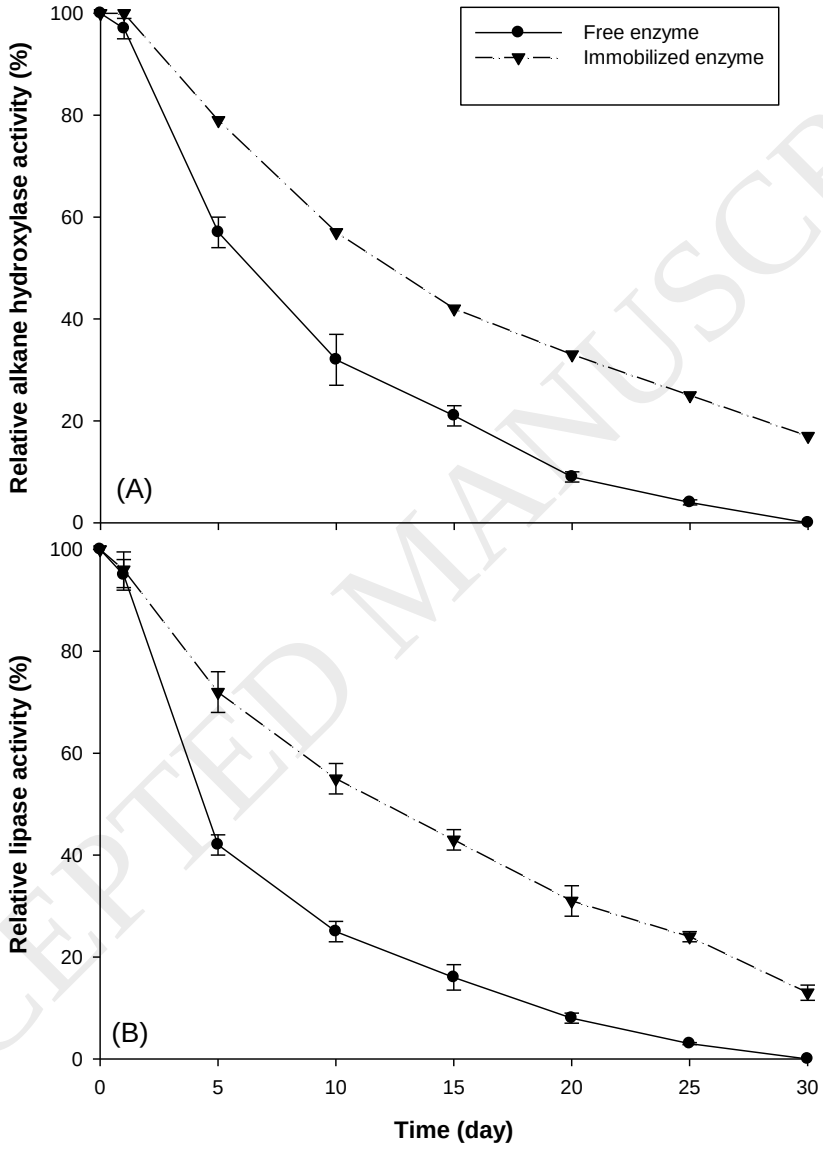

Fig. 5. In vitro half-life of the free and immobilized alkane hydroxylase (A) and; lipase (B).